Modern Imaging Technologies in Toxicologic Pathology: An Overview

Xiaoyou Ying and Thomas M. Monticello

Toxicol Pathol 2006; 34; 815
DOI: 10.1080/01926230600918983

Toxicologic Pathology, 34:815–826, 2006

ISSN: 0192-6233 print / 1533-1601 online
DOI: 10.1080/01926230600918983

Modern Imaging Technologies in Toxicologic Pathology: An Overview

XIAOYOU YING AND THOMAS M. MONTICELLO

Drug Safety Evaluation, sanofi-aventis, Bridgewater, New Jersey 08807-0800, USA

ABSTRACT

Modern imaging technology, now utilized in most biomedical research areas (bioimaging), enables the detection and visualization of biological processes at various levels of the molecule, organelle, cell, tissue, organ and/or whole body. In toxicologic pathology, the impact of modern imaging technology is becoming apparent from digital histopathology to novel molecular imaging for in vivo studies. This overview summarizes recent progresses in digital microscopy imaging and newly developed digital slide techniques. Applications of virtual microscopy imaging are discussed and compared to traditional optical microscopy reading. New generation digital pathology approaches, including automatic slide inspection, digital slide databases and image management are briefly introduced. Commonly used in vivo preclinical imaging technologies are also summarized. While most of these new imaging techniques are still undergoing rapid development, it is important that toxicologic pathologists embrace and utilize these technologies as advances occur.

Keywords. Bioimaging; digital microscopy imaging; virtual microscopy; digital pathology; in vivo preclinical imaging; automated microscopy imaging.

INTRODUCTION

Biomedical imaging (bioimaging) is defined as the multi-dimensional detection, characterization and visualization of biological processes. A bioimaging method should be able to obtain biological information in two (x, y) or three (x, y, z) morphological dimensions. A fourth dimension is added for a time course study (t). Imaging signal wavelength (λ) is also a critical dimension (Figure 1). Various imaging technologies have been developed using different signals along with the electromagnetic spectrum (Hendee and Ritenour, 2002; Suetens, 2002; Jerry et al., 2005), such as radio frequency for magnetic resonance imaging (MRI), visible light for optical microscopy, X-ray for computed tomography (CT) scans, and gamma ray for positron emission tomography (PET) imaging.

Pathology is a visual science predominantly based on light microscopy imaging. Applied light microscopy techniques have greatly advanced our knowledge at the cellular and tissue level resulting in the establishment of modern pathology (Malkin, 1998; Piller, 2001; Crawford, 2003). Other bioimaging technologies with clinical applications have been developed over the past decades mainly due to the innovation of computed tomography (Seeram, 1994; Bushberg et al., 2002; Oakley, 2003). Meanwhile, light microscopy imaging techniques with biological applications continue to develop due to innovations of novel fluorescence probes, confocal microscopy, automated microscopy and digital imaging. (Shotton, 1993; Wootton, 1995; Giuliano and Taylor, 1998; McCullough et al., 2004; Pawley, 2006). This overview will summarize the recent advances in digital pathology microimaging, digital slide scan techniques, virtual microscopy imaging, and new generation digital pathology platform approaches. In addition, in vivo preclinical imaging technologies is discussed briefly.

Address correspondence to: Xiaoyou Ying, PhD, sanofi-aventis, BRW JR2-103A, PO Box 6800, Bridgewater, NJ 08807-0800, USA; e-mail: xiaoyou.ying@sanofi-aventis.com, or Thomas M. Monticello, DVM, PhD, Merck and Co., PO Box 4, West Point, PA, 19486, USA; e-mail: thomas_monticello@merck.com

DIGITAL MICROIMAGING FOR PATHOLOGY

Digital pathology imaging encompasses the production, storage and retrieval of pathology image data. Advantages of digital imaging for microphotography in pathology are many. For example, pathology images in digital format can be identically reproduced, readily transferred and managed. The digital image data is natively appropriate for computer analysis, since the images are already in digital format. Recent advances in digital microimaging have improved digital microphotography quality, reduced equipment cost, and made the process more user-friendly.

A key device in digital microimaging is the digital camera system that usually consists of a digital (video) camera, a computer, a digital image input device, imaging software, and an optical connector to the microscope. Some older systems may employ an analogue camera with a frame grabber, but modern systems mostly employ a USB, Firewire, Gigabit Ethernet, Camera Link, or specific PCI interface. A camera that can be easily utilized to produce photo-quality images is a basic requirement for a digital microscopy system. A digital camera for pathology microimaging should have the following: (1) a large color dynamic range to ensure true-color fidelity, (2) high spatial resolution to match optical microscopy resolution, (3) high image acquisition rate to allow real-time or near-real-time view, (4) high speed data transfer, (5) a simple connection to a light microscope, and (6) ease of use (Table 1). Although an ideal digital camera that matches all of the above requirements is not yet available, some commercial products are now fairly easy to use and can produce images with satisfactory quality.

Digital microimaging is not only dependent on a high quality digital camera. All components in the pathway from the light microscope to the image display monitor (or printer) can decrease image quality and reduce digital imaging performance. For example, microscopic shading artifact is a

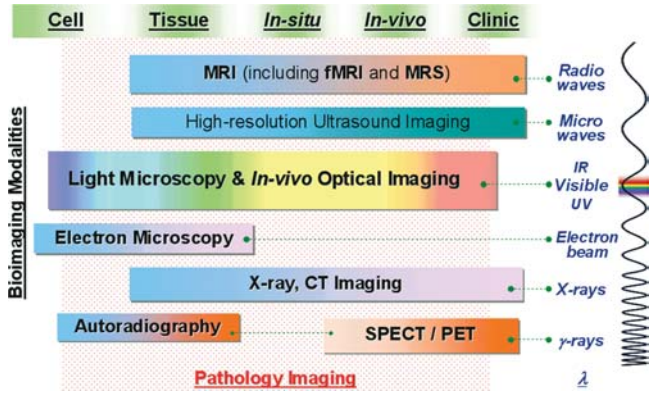

FIGURE 1.—Modern imaging modalities in biomedical research. Bioimaging technologies, which employ various signals in the electromagnetic spectrum, play a critical role in pathology.

commonly encountered problem with low magnification images since digital imaging is more sensitive than the human eye to non-uniform illumination. While digital image processing is able to help reducing illumination artifact, more uniform background imaging is now possible with microscopic components designed for digital microimaging (e.g., the Nikon "fly-eye" lens-array) (Drent, 2005).

The display of digital images is also critical in digital pathology microimaging. Although current high-end monitors are still not sufficient for ultra-high resolution pathology imaging, newly developed high-definition color monitors, such as the multi-mega-pixel true-color flat panel digital LCD monitors for diagnostic imaging, can display true-color pathology images with acceptable quality and affordability (Samei, 2005; DiIulio, 2006).

As advancements continue in digital imaging, it is clear that this technology is rapidly replacing conventional film for histopathology image capture. It is important to note, however, that while digital microimaging is becoming more common, standard operating procedures are still lacking for specific technical details including imaging system calibration, image compression, recommended image file formats, and image data management. These specifics will need to be addressed prior to routine application of digital imaging in GLP regulated studies. Although there is a lack of standards, progress is occurring, such as recommendations on the TIFF (Tagged Image File Format) and DICOM (Digital Imaging and Communications in Medicine) file formats for scientific/medical images, and multiple studies have shown the acceptance of the lossy image compression and JPEG image format for pathology images with certain restrictions (Okumura et al., 1997; Felten et al., 1999; Ying and Chung, 1999; Molnar et al., 2003; Rossner and O'Donnell, 2004; Tengowski, 2004; Conrath et al., 2006). We can anticipate more efforts in the near future on establishing additional recommendations and standards for pathology imaging.

AUTOMATED WHOLE SLIDE IMAGING AND VIRTUAL MICROSCOPY

While digital microphotography significantly enhances the capability of recording and sharing histopathology findings, it can still be time consuming to calibrate a digital microscopy imaging system and acquire standardized images manually. During the past 2 decades, various automated microscopy imaging techniques have been developed for entire tissue sections or whole tissue slides (Preston, 1986; Ying, 1995; Felten, 1999; Steinberg and Ali, 2001; Leong and Leong, 2004).

In general, automated microscopy imaging techniques for digitizing an entire slide utilizes one of the following three basic slide scanning technologies: (1) *Automated area-scan microimaging* (via a CCD camera), which involves 'tile-by-tile' acquisition over the entire tissue section followed by a stitching of images to form an entire digital slide, (2) *Automated 1D line-scan microimaging*, which consists of linear scanning of small tissue section areas to form a 'strap image' with further stitching of the straps to form a digital slide, and (3) *Array microscopy imaging*, in which the lens-array parallel scanning of an entire slide to form is used a whole slide image using a specially designed microlenslet array and a large 2D imaging chip.

Automated Area-Scan Microimaging: In principle, the automated area-scan microimaging technique is not much different than conventional digital microscopy imaging and mainly employs autofocusing, automated mechanical shift, digital image acquisition, and large image formation techniques to obtain a whole digital slide. This method allows integrating components of well-designed optical microscope and high-end CCD camera. With the inherently fixed pixel registration in x, y dimensions, area-scan microimaging can provide a high-quality image and permits the flexibility to employ specific light microscopy methods. However, the area-scan process may take a long time (~5 to >60 minutes) to create the entire digital tissue section/slide since a large number of individual images (at high resolution) are needed. Recently, newer techniques have been developed that significantly improve scanning speed, such as

TABLE 1.—Ideal and practical specifications for digital camera in pathology microscopy imaging.

Key issues	Ideal parameters required in pathology microscopy imaging	Practical specifications currently applicable in pathology microscopy imaging
Digital imaging resolution	≥12–16 Mega-pixels to match the 35 mm film photo resolution; and match the perfect optical microscopic resolution	~2–12 Mega-pixels per single image
Color fidelity	≥10 bits per color for 3 primary color (RGB) to produce true-color microscopic image	3 CCD, or single CCD with color filter, for 3 × 8 or 3 × 10 bits RGB true color imaging
Image display	≥25 frame/s (video rate) display for real-time viewing with display resolution of 1280 × 1024 or better	~10–15 frame/s with display resolution of 1024 × 768 or better
Image archiving	<1sec for fast image transferring and saving; lossless image archiving	~1–5 sec in image transferring and saving; lossless compression, or lossy compression with visually lossless result
Easy to use	Turnkey operation with automated exposure, white balance, shading correction, image archiving, etc.	Turnkey operation with automated exposure, computer-assisted white balance, shading correction, image archiving, etc.

improved precision to scan the tissue sections only (Wetzel et al., 2006).

Automated 1D Line-Scan Microimaging: Unlike automated area-scan microimaging, which combines electronic scan within the imaging field and mechanical scan to shift the imaging field, the line-scan utilizes a 1D linear CCD sensor to mechanically scan the slide to form image strips. Since a long image strip covers a much larger imaging area than that of a single image, this method can form an entire slide with less single image stitching time, which increases the imaging speed. In addition, the optical signal is acquired line-by-line so a correction is not needed for the scanning axis dimension. However, for the line-scan method, it is a challenge to ensure the accuracy of individual micro-area focusing and line-to-line image registration, which could decrease image quality, especially at high magnification.

Array Microscopy Imaging: This method uses multiple miniature microscopic objectives and parallel digital image acquisition and processing to rapidly scan a whole slide. Although the idea is straightforward, there are many technical challenges. To date, only one technique has been developed and commercialized for automated tissue slide microimaging (Olszak and Descour, 2005). The key device is a 2D array of 8 × 10 miniature microscopic objectives overlaid by a specially designed CMOS imaging sensor (Weinstein et al., 2004, 2005). This miniature digital-optical microimaging device can produce image data in the form of 80 strips simultaneously, so one scan of the slide could form an entire digital slide. Due to the fixed precise arrangement of the optic/imaging-sensor elements, all strips are stitched together during the scan. With the parallel optical-digital imaging approach, an ultrarapid scan (∼58 sec) of an entire slide can be achieved (Weinstein et al., 2004). A weakness of this ultrarapid automated scanning with fixed miniature objectives is the difficulty ensuring accurate local focusing. In addition, the CMOS sensor may also limit further improvement of image quality.

Requirement for Toxicologic Pathology and Automated Whole-Slide Microimaging Systems: Toxicologic pathologists primarily utilize the light microscope with 0.5–40 × objective lenses, so with this magnification range, any of the three automated microimaging techniques could be utilized. Currently there are more than 10 different automated microscopic imaging systems commercially available for digitizing an entire tissue slide, including single slide based low-cost systems (e.g., the BLISS Slide Scanner, Bacus Laboratories, IL, and the CoolScope VS, Nikon, NY) and mid-high throughput multi-slide systems (Table 2). For low through put applications and personal use, a simple automated microimaging system with one to a few slide capacity is an option, since low scan speed (e.g., ∼2–3 slides per hour) would be acceptable. For greater needs (e.g., pathology department), a mid-throughput automated micro-imaging system, with slide-handling capacity of ∼50 to 500 slides, may be adequate. A high-throughput automated microimaging system would be needed for establishing a complete digital pathology workflow for routine studies on a day-to-day basis.

Virtual Microscopy Reading: A direct impact of automated microimaging technology is that digital (virtual) slide data can be made available to pathologists to permit evaluation (reading) of tissues without the use of a personal microscope (VMR, virtual microscopy reading). With appropriate spatial and color/intensity resolutions, a digital slide could virtually represent the original glass tissue slide. Therefore, diagnosis based on the virtual slide could be acceptable (Costello et al., 2003; Molnar et al., 2003; Kumar et al., 2004; Helin et al., 2006).

To validate this acceptance in toxicologic pathology, we conducted a comparison evaluation of routine H&E stained rat tissue slides using the VMR and conventional optical microscopy reading (OMR) methods (Ying et al., 2004). In this validation study, an automated digital slide area-scanning system (MedScan, Trestle Corp., CA) was employed to digitize glass tissue slides in order to obtain the virtual slide data sets. The system consisted of an autofocusing multi-slide scanning mechanism (Trestle Corp), a modified optical microscope with 4 × /0.10, 10 × /0.50 and 20 × /0.70 objectives (Olympus, Japan) and a 3 CCD digital camera (JAI Inc., CA). For this study, 300 H&E stained rat tissue sections from 8 rats (4 males and 4 females, ∼20 slides each) were digitized. Data sets were created by scanning the entire tissue sections on glass slides, image-by-image. The sampling resolution for tissue image digitization was 0.32 μm/pixel (for spatial resolution of ∼0.64 μm), and the color depth was 3 × 8 bits (true RGB via a 3 CCD). This is virtually equivalent to conventional optical microscopy using a 40 × /0.70 objective lens. The partial tissue images were then stitched together to form a single digital slide image with different resolutions in multilays. JPEG compression was utilized to reduce the digital slide image size. The compression ratio for the whole slide images ranged from 15:1 to 40:1 (this variability was attributed to the tissue image content). The average digital slide image file size was ∼500 MB per slide (ranging from 300 MB to ∼1.2 GB, depending on the size of the tissue section). All digital slide data were stored in a 4TB image data server that was accessible via an intranet.

Four pathologists assessed and agreed upon the quality of the digital slides prior to the evaluation. The virtual digital slides were then evaluated (read) by one pathologist on a personal pathology image view station (Dell 340 Precision workstation equipped with dual 19" flat-panel LCD monitors, Dell Inc. TX), via our intranet, with a Windows-based virtual microscopy reading software (MedScan Viewer, Trestle Corp) as shown on Figure 2. The basic tools used by the pathologist to conduct the VMR were just a regular computer mouse and keyboard. Microscopic findings were entered into a computer using the PathData software (Pathology Data Systems Inc., CA).

A fully automated light microscope (Eclipse E1000M, Nikon, Japan) was used for the OMR to avoid any favorable bias on the VMR. Automated functions of the light microscope included auto-link focusing, motorized nosepiece and condenser, and the auto Koehler illuminating system that consisted of motorized field and aperture stop and motorized continuous ND filters (ND1 to ND8).

Comparison of the VMR and OMR: The same tissue slide sets in both formats (glass slide and digital slide) were

TABLE 2.—Commercially available automated whole-slide imaging systems (based on current information from public sources and manufacturers. This is an uncompleted product list; the authors do not endorse any products or manufacturers).

	Aperio ScanScope System	Carl Zeiss MIRAX SCAN System	DMetrix DX-40 Scanner	Hamamatsu NanoZoomer Digital Pathology Slide Scanner	Trestle DSM System
Microscopy scanning technology	1D CCD line Scan	Microscopic area-scan imaging with 2D CCD	10 × 8 lenslet miniature array microscopy with 2D CMOS	1D CCD line Scan	Microscopic area-scan imaging with 2D CCD
Imaging sensor	2098 line CCD sensor (trilinear array)	1032 × 776, or 1380 × 1024 1/3" progressive scan IT CCD	Dmetrix DM5760 CMOS image sensor, =24 megapixel	4096 × 64, 3 CCD TDI sensor	3 CCD digital color camera, 36 bit
Slide scanning resolution (sampling resolution, μm/pixel)	0.5 with 20× obj. (0.75NA) and 0.25 with 40× obj. (0.75NA)	0.37 with 20× obj (0.8NA, 0.63× mount) and 0.18 with 40× obj (0.95NA, 0.63× mount)	0.47 with the miniature objectives (0.6 NA)	0.46 or 0.23 selectable, with 20× obj. (0.70 NA)	0.47 at 20× mode, and 0.23 at 40× mode (0.75NA obj)
Slide scanning speed	~3min with 20× obj. for 15 × 15 mm^2 (with slide setup time)	~5min with 20× obj. and 0.63× mount for 15 × 15 mm^2	~ 40 slides per hour (58 seconds for 15 × 15 mm^2) Minimum scanning rate: 17 slides/hour for full slide area.	~5min at 0.46 μm/pixel resolution ~14min at 0.23 μm/pixel, for 20 × 20 mm^2	~5min with 10× obj. for 20× equiv.; ~15 min with 20× obj. for 40× equiv. for 15 × 15 mm^2
Autofocusing method	Prefocus map augmented by interstripe autofocus	Image based autofocus during scanning	Topographic focusing, based on an automatically calculated trajectory	prefocus-map	Volume Scan using z-stack; Surface Scan using pre-focus map
Number of objective Positions	1 (optical doubler doubles resolution at the CCD)	1 (with option to add magnification multipliers)	N/A—micro-lenslet based	1 (20× or 40× scanning option available with single objective)	6 (2×, 4×, 10×, 20×, 40×, 60×)
Multi slide handling	Automatic, 120 slides maximum	Automatic, 300 slides maximum	Automatic, 240 slides maximum	Automatic, 210 slides maximum	Automatic, 50 slides maximum
Image compression	JPEG or JPEG2000 compression	JPEG compression	JPEG compression	JPEG compression	JPEG compression
Virtual slide file Format	Standard TIFF 6.0 based .svs format, w JPEG/JPEG2000	Pyramidal file format / JPEG compressed image tiles	JPEG based	JPEG image format plus slide information	Standard TIFF 6.0 /JPEG
Barcode slide management	Yes, multiple 1D and 2D barcodes	Yes, 1D Standard; 2D optional	Yes, 1D and 2D codes supported	Yes, 1D standard; 2D optional	Yes, multiple 1D and 2D barcodes
View software solution	Yes. ImageScope	Yes. Mirax Viewer	digitalEyepiece; Iris™ web-browser viewer	Bacus Labs viewers-ActiveX, Java, WebSlide Browser	Yes. MedMicroscopy and Xcellerator DSS
Slide management Software	Yes. Spectrum (Rel 8) Workflow Manager (slides & associated data)	No	Yes, offered with third parties: Apollo Telemedicine PathPACS™ and BioImagene SIMS™	Yes. WebSlide Finder & SlideTray	Yes. Xcellerator DSS; MedDS, etc. (slides, images, and case data)
Telepathology software solution	Yes, live display and Z stack "revisit mode"	Yes, virtual slide based.	Yes, virtual slide based, offered with third party: Apollo Telemedicine PathPACS	No. (remote viewing available)	Yes. Advanced function with MedMicroscopy or Xcellerator DSS

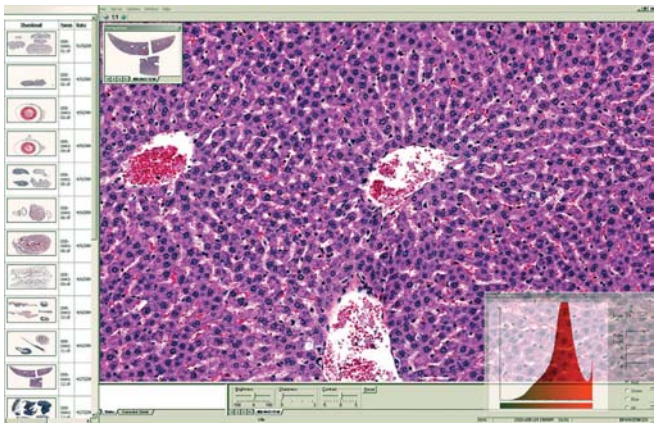

FIGURE 2.—A screen picture illustrates the Windows-based VMR of a digital slide. This method was used for the VMR trial on a set of toxicologic pathology slides.

reviewed for the comparison. Similar diagnostic results were obtained with both VMR and OMR, including similar severity and incidence rates (Ying et al., 2004). Other studies reported in the literature have also shown high diagnostic corresponding rates for virtual microscopy and conventional microscopy readings (Steinberg and Ali, 2001; Molnar et al., 2003; Gagnon et al., 2004; Lundin et al., 2004).

Another result from this comparison study is that there was no significant difference in the time needed to evaluate the complete set of images (slide-reading time) between OMR and VMR in this trial. It should be noted, however, the comparison of VMR vs. OMR was performed with some bias favoring OMR: (1) OMR was performed on a high-end automated optical microscope that did not require manual adjustment of the light condenser or objectives, (2) VMR was conducted on a typical desktop pathology workstation using standard quality flat-panel monitors, and (3) the pathologist was very experienced using OMR but had little experience

TABLE 3.—Optical microscopy reading (OMR) vs. virtual microscopy reading (VMR).

Features/Functions	OMR method	VMR method
Slide searching speed	**B:** (minutes)	**A:** (seconds to minutes)
Convenience of slide handling	**C:** physical	**A:** digital (virtual) slide
Slide management	**B:** physical	**A:** digital slide database
Working condition (ergonomic)	**C:** under light microscope	**B:** large high-quality monitor
Tissue image quality	**A:** best	**B:** depends on digital microimaging equipment
Cost-slide storage (per slide)	**A:** <$1?	**B:** <$1 (A: lower in long term)
Cost-personal system	**C:** high-quality microscope	**B:** high-end PC
Cost-slide scanning server	**A:** no need	**B:** digital slide imager
Work portability	**C:** microscope needed	**A:** anywhere with PC & network access
Slide data sharing and peer review	**C:** physical relocation needed	**A:** anywhere with PC & network access
Quality Control	**B:** Evaluation of whole slide needed by technician/pathologist	**A:** automation possible
Slide photography	**B:** microscopy photography	**A:** digital copy and paste, standardized
Comparative view of multiple slides	**C:** special microscope needed	**A:** easy with multiple view windows
Concurrent review by multiple people	**C:** multi-head microscope needed	**A:** easy with network connected telepathology
Computer-aided analysis	**C:** further processing needed	**A:** digital image ready for analysis

A = Excellent; **B** = good; **C** = acceptable; **D** = unacceptable; OMR = Optical Microscopy Reading; VMR = Virtue Microscopy Reading.

with VMR and the software. It would be anticipated that "slide read time" would decrease with more experience using VMR and, in fact, significantly higher slide reading speed was shown with virtual slides in several clinical pathology studies (Molnar et al., 2003; Weinstein et al., 2004; Burthem et al., 2005).

As the comfort level of VMR increases with pathologists, this approach obviously has many advantages (Table 3). These advantages include the creation of centralized histopathology and standardized digital scan processing laboratories, and instant worldwide 'distribution' of virtual slides to offsite pathologists, peer review pathologists, and consultant pathologists via the Internet.

NEW GENERATION DIGITAL PATHOLOGY APPROACHES

Tissue slides in digital form, combined with VMR, can provide pathologists great flexibility and efficiency. In fact, a major benefit with digital slides is that the fully digitized tissue slide data can be directly linked to computer-assisted pathology image data analysis (e.g., digital morphometry). We designed a digital pathology imaging workflow to actually take advantages of these technologies (Figure 3). The first step involves converting glass tissue slides into a digital format by use of automated whole-slide microimaging. The second step establishes a central digital slide database for slide management and virtual slide access. Additional features, such as computer-assisted quantitative image analysis, can be added to provide objective/quantitative information when needed. Fully automated prescreening of digital tissue slides may also be achieved in the future.

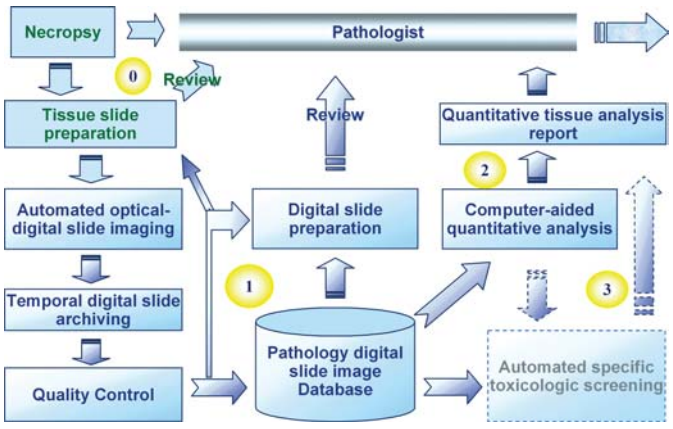

FIGURE 3.—Designed new generation digital pathology workflow.

Automated Slide Inspection: An immediate benefit from digital pathology is the capability for automatic quality control slide inspection—namely, digitally screening slide images for staining quality, proper tissue layer (i.e., lack of folds and tears) and thickness, as well as the presence of any other artifacts. This process can then determine unacceptable slide quality prior to the review by the pathologist. Automated slide inspection could also be used for automated tissue classification and validation—identifying tissue types, validating slide labels and/or classifying slides for the digital slide database.

Pathology Image Management and Digital Slide Database: Pathologists need a tool to manage pathology image data. Unfortunately, there is still no ideal solution that is widely accepted. Why is it so difficult to develop a user-friendly pathology image database management system? One major reason is that pathology images are not in single or simple data formats (types), and usually have no inherent context, which requires supporting text data (or data in other formats) along with the image data to make them interpretable or meaningful.

Although a database system for management of manually captured single images is needed, an efficient solution for image management is with whole digital slide-based data. A digital slide contains hundreds or thousands of regular sized images that stitch together to form the entire tissue section. The image location index is natively embedded in the digital slide. Within a digital slide, fields (images) of interest can be easily marked and retrieved. Thus, a digital slide image database could manage large amounts of images and more logically organize pathology images per project or per study (Figure 4).

Currently there are still many challenges for digital slide based image data management, such as generating and managing extremely large data volumes of high-resolution whole slide images, transferring large amounts of data over the network (at least ~512 kbps is needed for practical use), and the lack of standards. Another challenge that needs to be addressed when VMR is utilized in nonclinical toxicology studies is compliance with the Code of Federal Regulations

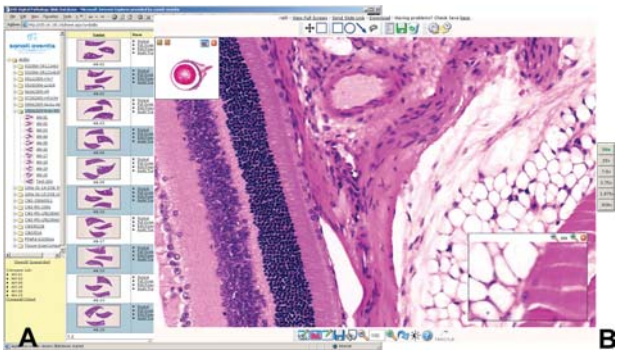

FIGURE 4.—A screen picture illustrates the Web-based digital slide database (A) and Web-based virtual microscopy view (B).

(CFR), Volume 21, Part 58 (Good Laboratory Practices [GLP]) and Part 11 (Electronic Records/Signatures).

Quantitative Analysis and Computer-Assisted Image Data Mining: Conventional evaluation of tissue slides is based on visual analysis of the light microscopic image. The interpretation based on this microscopic observation very much depends on the pathologist's subjective view and decision-making capability, which is based on the pathologist's theoretical knowledge, experience, analytic and associative abilities. One promising concept moving forward is to use computerized artificial intelligence and whole digital slide data sets to automatically screen slides and differentiate them as normal or abnormal. Using automatic detection, resources could be utilized more efficiently by having the pathologist first only review images binned as abnormal. Several initial studies have demonstrated the advantages of this strategy (Kriete and Boyce, 2003, 2005; Johnson and Braughler, 2003) and software prototypes from the industry have been, or are currently in development (e.g., Definiens AG, Germany; BioImagene Inc., CA; and Systems Pathology Company, LLC, MD). These automated pathology solutions could be very useful for high content analysis, aimed at well-defined specific lesions. Eventually, automated pathology and high content analysis could be used for prescreening of tissue specimens in toxicologic pathology. However, this technology has not yet reached maturity, especially for comprehensive tissue lesion determination. Although it is theoretically and technically achievable, the development of specific algorithms/assays for a wide base of tissues and abnormalities will take a tremendous effort in the algorithm/assay and software development.

A more readily achieved solution is to develop a simple and efficient tissue slide analysis tool to enable the pathologist to take advantage of digital slide data sets and advanced digital image analysis methods. We designed a new approach of "pathologist-supervised self-learning lesion detection" (Figure 5). The strategy is to combine the knowledge and expertise of the pathologist with the computer capability of repeating image content search/analysis to detect all pathologist-defined patterns (lesions or abnormalities), and/or to conduct quantitative analysis over whole pathology tissue sections. Based on our initial proof-of-concept study, this strategy could be more quickly developed and applied in toxicologic pathology.

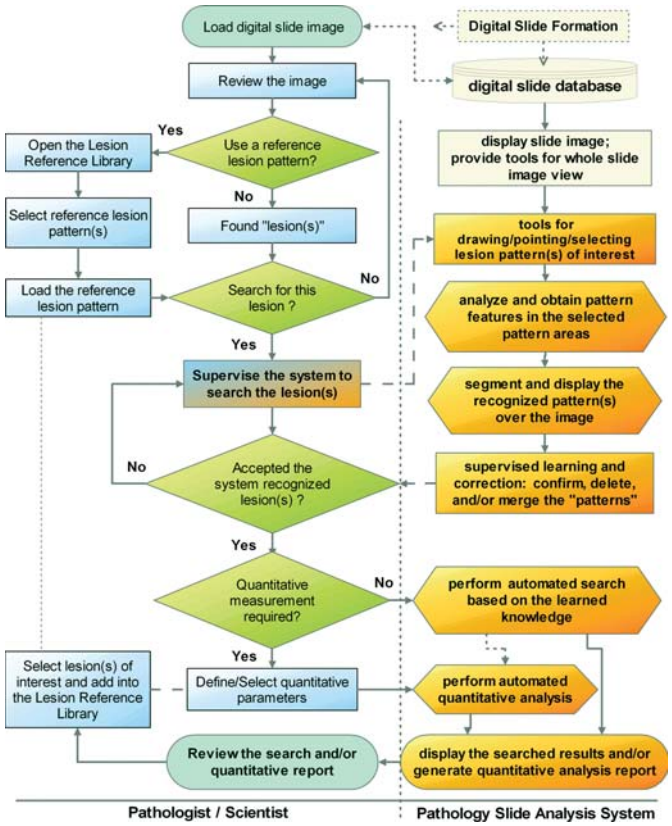

FIGURE 5.—Diagram outlines the pathologist-supervised, self-learning lesion detection method.

Fully automated pathology analysis technologies will not be popular in the near future due to time-consuming and costly development. The widely available image analysis technology today is still the low-cost "toolbox" based image analysis packages, such as the Image-Pro Plus (Media Cybernetics, Inc., MD), PAX-it (MIS Inc., IL), AxioVision (Carl Zeiss, Germany), and NIH Image or Image-J, (NIH, MD). New features in these "toolbox" approaches are mainly the improved functions and user interface. Some software programs can now process and analyze ultra large images, even for entire digital slides. As more specific methods/assays are developed and embedded in the software packages, the toolbox-based solution will continue to be an effective instrument for toxicologic pathology applications.

Although pathology microimaging is mainly based on brightfield microscopy of H&E stained specimen, various specific optical microimaging techniques may also benefit pathologists for detection and localization of cellular/molecular signatures in tissue. These emerging or validated optical imaging techniques include Raman spectroscopy imaging for highly detailed chemical information of tissue sample, spectral reflectance imaging for identifying some tissue/cell abnormal variations (e.g., cancer), 2-photon and other confocal microimaging techniques for ultrathin tissue (virtual) sectioning and 3D microimaging (Baena and Lendl, 2004; Rubart, 2004; Singer et al., 2005; Chung et al., 2006; Pawley, 2006). As demonstrated in Figure 6, 2-photon/single-photon confocal immunofluorescence microscopy was applied on a mouse brain tissue slide

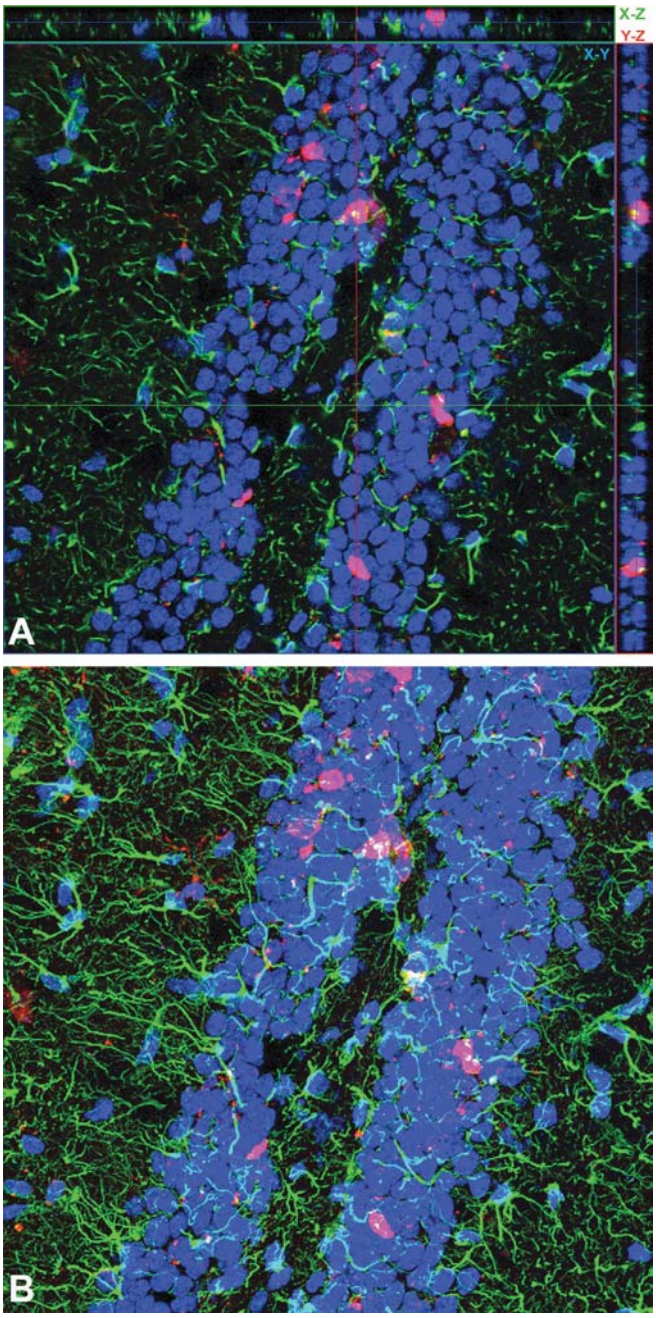

FIGURE 6.—Two-photon/one-photon confocal immunofluorescence microscopy image of a brain tissue section from an inflammation mouse model. Green color indicates the astroglial marker GFAP (Glial Fibrillary Acidic Protein), red illustrates the macrophages/microglia immunodeteced by the F4/80 (antiserum against the macrophage antigen) antibody, and blue shows cell nuclei labeled by Hoechst 33342, a dsDNA-interactive agent. The brain section is 12 μm-thick and further optically sectioned to 33 sub-sections. Figure 6A), the X-Y, X-Z, and Y-Z sectioning view of a $230 \times 230 \times 12\ \mu m^3$ 3D image data cube. Figure 6B), the 3D reconstructed image.

to obtain highly accurate, 3D colocalization information of the cells/proteins of interest. For quantitative immunohistochemistry, molecular pathology, and systems pathology applications, many of these emerging techniques could be included into the new generation digital pathology approach.

IN VIVO PRECLINICAL IMAGING

Preclinical imaging, i.e., animal imaging that could directly bridge to clinical imaging, has made great advances over the past decade. The capacity to detect and visualize biological and pharmacological processes in vivo at cellular and molecular levels in animals may also provide a unique tool to observe in vivo pathological alterations. Modern preclinical imaging modalities include high-resolution animal MRI (or magnetic resonance microscopy), high resolution X-ray micro-tomography (micro CT), positron emission micro-tomography (micro PET), animal single photon emission computed tomography (animal SPECT), ultrasonic microscopy imaging, and in vivo optical imaging (Figure 7 and Table 4).

Animal MRI: Animal MRI was applied to toxicologic pathology prior to the preclinical imaging concept being well developed (Johnson and Maronpot, 1989; Delnomdedieu et al., 1996; Maronpot et al., 2004). It is now well recognized that animal MRI could be an excellent experimental tool for the detection of pathologic alterations in soft tissues, as well as an adjunct in vivo screening method to monitor the genesis, progression, or regression of chemically induced lesions repeatedly in the same animal (Dixon et al., 1988). Based on animal MRI studies in toxicologic pathology (Hedlund et al., 1991; Zhou et al., 1994; Delnomdedieu et al., 1998), a new concept of magnetic resonance histology (MRH) has been developed (Johnson et al., 2002). MRH offers a nondestructive approach and is uniquely specific to MRI biomarkers in 3D. Animal MRI technology not only provides in vivo fine anatomic contrast resolution in soft tissue imaging but also can detect to alterations in the chemical and physical microenvironment of the tissue. In preclinical studies, animal MRI is becoming a powerful in vivo imaging tool to measure compound-induced pathophysiologic changes in soft tissue organs such as the liver, brain, cardiovascular system, kidney, and reproductive organs. For example, animal MRI has been demonstrated to be a useful tool to measure hepatic steatosis, quantify liver fat/water ratios, rat brain lesion, and noninvasively monitor for possible compound-induced toxicity, etc. (Weiss et al., 1994; Schmitz et al., 1996; Hockings et al., 2003; Preece et al., 2004; Zhang et al., 2004; Tengowski and Kotyk, 2005).

X-ray Imaging and Micro CT: X-ray imaging and micro CT can be useful for visualizing and measuring

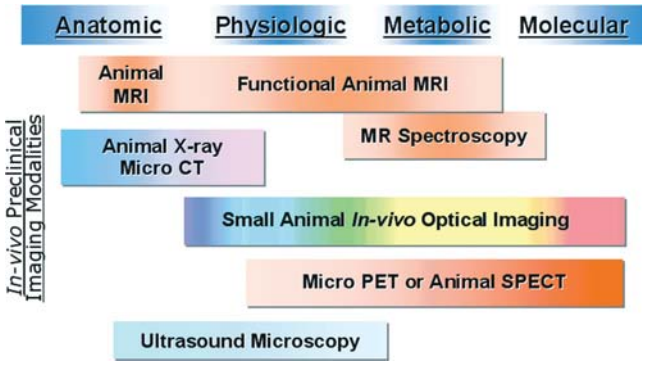

FIGURE 7.—Commonly used preclinical imaging modalities.

TABLE 4.—In vivo preclinical imaging modalities.

Preclinical imaging technology	Primary application	Resolutions	Molecular sensitivity	Commonly used imaging agents	Specifics in toxicologic pathology	Limits
Animal MRI	Anatomic imaging of soft tissue organs, and functional imaging	x, y, z: ~10–100 μm (no limit in depth) t: minutes-hours	Low-Mid	Gadolinium, UPSIO, etc.	MR histology, tumor, fat/water, etc. Non-invasive imaging study	Limited molecular imaging applications, long scan/processing time needed
Micro CT	Anatomic imaging of lung, bone, tumor, etc.	x, y, z: ~10–50 μm (no limit in depth) t: minutes	Low	Iodine	Bone lesion, non-invasive imaging study of tumor and lung, etc.	Limited molecular imaging applications, poor soft tissue contrast, radiation
2D Fluorescence imaging	Imaging of molecular events, e.g., protease imaging	x, y: ~1–4 mm z:n/a (depth<~20 mm) t: seconds-minutes	High-Ultrahigh	Near-infrared fluorochromes, Fluorescent proteins	In vivo molecular /functional imaging study of pathology alterations	Low spatial resolution, limited depth imaging
2D Bioluminescence imaging	Gene expression, cell tracking, etc.	x, y: ~2–4 mm z:n/a (depth<~25 mm) t: seconds-minutes	Ultrahigh	Luciferin	In vivo molecular imaging study of pathology alterations	Not applicable to clinic, low spatial resolution, limited depth imaging
Animal/organ intravital fluorescence microscopy	Gene expression, cell tracking, molecular localization, protein-protein interaction, etc.	x, y: ~0.2–1 μm z: ~0.7-1.2 μm (depth<~500 μm) t: sub-seconds-minutes	High-Ultrahigh	Fluorochromes, Fluorescent proteins, Fluorescent-labeled antibodies, Quantum dots, etc.	Cellular, molecular and functional imaging study of pathology alterations	Invasive very limited depth imaging; low throughput
Micro PET	Metabolic, Molecular & functional imaging; receptor/ligand binding	x, y, z: ~1.2–2.5 mm (no limit in depth) t: minutes	Ultra-high	F-18 FDG, Carbon-11, Oxygen-15, etc.	In vivo molecular /functional imaging study of pathology alterations	Difficult and high cost radiolabeling, low anatomic resolution, radiation
Animal SPECT	Metabolic & functional imaging with tracers; receptor/ligand binding	x, y, z: ~1–2.5 mm (no limit in depth) t: minutes	High	Technetium-99, Iodine-123, Indium-111.	In vivo molecular /functional study of pathology alterations	Low anatomic resolution, limited applications
Ultrasound microscopy	Real-time morphological imaging of soft-tissues, e.g., cardiovascular imaging	x, z: ~40–80 μm (depth = mm); y: n/a for 2D UI t: sub-seconds	Low	Micro-bubbles	Noninvasive monitoring of path-morphological alterations	Mostly morphological analysis only, limited spatial resolution

pathologic alterations of lung and bone micro-architectures (Ritman, 2002; Lee et al., 2003; Barck et al., 2004; Langheinrich et al., 2004a), organ vasculature (Langheinrich et al., 2004b; Ritman, 2005), and morphologic quantification of tumors (De Clerck et al., 2004; Gasser et al., 2005). For instance, as a traditional utilization of X-ray imaging, micro CT is a key approach for evaluation of lung pathology changes such as emphysema in mice (Postnov et al., 2005). Similar to animal MRI, micro CT allows intact organ, even the whole intact animal, to be studied in vivo. Especially, the non-invasive in vivo 3D imaging capacity of micro CT can provide highly accurate 3D morphologic analysis, such as in vivo measurement of mouse lung airway wall (Nixon et al., 2005) and mouse heart chambers (Badea et al., 2006).

Micro PET and Animal SPECT: Unlike animal MRI and micro CT, micro PET and animal SPECT are not able to provide high spatial resolution for anatomic structures. However, PET/SPECT's unique capacity of quantitatively and noninvasively detecting physiologic concentration of radiopharmaceuticals in vivo, combined with the ultrahigh sensitivity in visualization of interested molecular location and activities, has resulted in many applications in preclinical studies. Currently, applications of micro PET and animal SPECT imaging include organ perfusion (e.g., cerebral blood flow), glucose or oxygen metabolism, gene expression, tracking of neurotransmitter and receptors, neural activation, tumor angiogenesis, hypoxia and apoptosis (Gambhir et al., 2000; Myers, 2001; Herschman, 2003; Laforest et al., 2005; Wang and Maurer, 2005; Yee et al., 2005).

In vivo Optical Imaging: In vivo (molecular) optical imaging for small animals includes in vivo bioluminescence imaging, in vivo near-infrared fluorescence (NIRF) imaging, and in vivo fluorescent protein imaging. In vivo optical imaging can quickly detect transient organ functional events at the cellular and molecular level, which aides in the measurement and understanding of pathological alterations within organs. Another advantage of in vivo optical imaging is specificity and accuracy; specific optical probes are readily available for labeling many biomolecules, structures, or cell types. Immunofluorescent probes can be directed to bind to specific proteins (antibodies, ligands, toxins). Through specifically engineered transgenic animals, very specific in vivo analyses can also be performed (Hoffman, 2005; Shah and Weissleder, 2005). Advances in biochromophores, like GFP mutants, can be used to identify and track specific proteins expressed inside living organs (Hoffman, 2002). Since in vivo optical imaging can be directly linked to the optical methods in molecular/cell biology (e.g., in vitro fluorescence microscopy), it plays a significant role in translating molecular/cell biology from in vitro to in vivo or in situ (e.g., in vivo validation). During the past years, in vivo optical imaging methods have been widely applied for studies on gene expression (Hoffman, 2002), infectious diseases (Contag et al., 1995; Benaron et al., 1997; Doyle et al., 2004), inflammation (Carlsen et al. 2002; Magness et al., 2004), metabolism (Malaisse, 2005), oncology and angiogenesis (Choy et al., 2003, Hoffman, 2004; Montet et al., 2005), in vivo protein-protein interaction (Welsh and Kay, 2005), and in vivo toxicology and chemical toxicity (Weir et al., 2005).

More advanced optical imaging techniques are rapidly being developed and applied to in vivo studies, such as the reflectance spectroscopy, 2-photon 3D microscopy, and multispectroscopy imaging methods we are now all applicable to in vivo (Hoffman, 2005; Chung et al., 2006; Haka et al., 2006; Pawley, 2006; Pinaud et al., 2006).

Currently, preclinical imaging technologies and applications are still in a rapid growth phase. New technologies, including micro PET/CT combination, microPET/MRI combination, and in vivo optical CT, are under development to provide both high anatomic resolution and molecular imaging sensitivity.

Summary

Pathology imaging capabilities can now extend from basic microscopy observation to include advanced digital pathology microimaging functions. These functions not only significantly improve manual image capture but, more importantly, enable automated and standardized entire slide imaging scan, and can convert conventional light microscopy to distance-free and microscope-free virtual microscopy. Modern digital microimaging technologies are becoming practical to pathologists.

Currently available digital microimaging technology is already sufficient to replace film in microphotography. With digital slide data available, major future applications in toxicologic pathology will be virtual microscopy reading, microscope-free micro-image capture, whole slide image sharing, and computer-assisted analysis. Digital slide data are also creating some novel approaches in toxicologic pathology, such as digital pathology platforms that may provide automated tissue slide quality control checks, whole slide image database and electronic slide management, and pathologist-supervised automatic lesion detection. Modern imaging technologies also enable molecular and/or functional imaging. These added capabilities extend ex vivo microscopic tissue observation to in vivo microimaging for whole body detection/visualization.

Many of the new imaging techniques presented in this review are still under rapid development. There is much work needed to embed these new methodologies into practical approaches such as establishing standard operating procedures and validating the new technologies. It is important that toxicologic pathologists embrace and utilize these new imaging technologies as advances occur.

Acknowledgments

We thank Dr. Bruce McCullough and Dr. Marc Bonnefoi for their valuable ideas and support. In addition, we thank our many departmental co-workers, especially Drs. Jean-Guy Bienvenu, Michael V. Pino, Norman J. Barlow, and Daniel Weinstock for their work in digital pathology applications.

References

Badea, C. T., Bucholz, E., Hedlund, L. W., Rockman, H. A., and Johnson, G. A. (2006). Imaging methods for morphological and functional phenotyping of the rodent heart, *Toxicol Pathol* **34**(1), 111–7.

Baena, J. R., and Lendl, B. (2004). Raman spectroscopy in chemical bioanalysis. *Curr Opin Chem Biol* **8**(5), 534–9.

Barck, K. H., Lee, W. P., Diehl, L. J., Ross, J., Gribling, P., Zhang, Y., Nguyen, K., van Bruggen, N., Hurst, S., and Carano, R. A. (2004). Quantification of

cortical bone loss and repair for therapeutic evaluation in collagen-induced arthritis, by micro-computed tomography and automated image analysis. *Arthritis Rheum* **50**(10), 3377–86.

Benaron, D. A., Contag, P. R., and Contag, C. H. (1997). Imaging brain structure and function, infection and gene expression in the body using light. *Philos Trans R Soc Lond B Biol Sci* **352**(1354), 755–61.

Burthem, J., Brereton, M., Ardern, J., Hickman, L., Seal, L., Serrant, A., Hutchinson, C. V., Wells, E., McTaggart, P., De la Salle, B., Parker-Williams, J., and Hyde, K. (2005). The use of digital 'virtual slides' in the quality assessment of haematological morphology: results of a pilot exercise involving UK NEQAS(H) participants. *Br J Haematol* **130**(2), 293–6.

Bushberg, J. T., Seibert, J. A., Leidholdt Jr., E. M., and Boone, J. M. (2002). *The Essential Physics of Medical Imaging* (2nd ed.), Lippincott Williams & Wilkins, Philadelphia, PA.

Carlsen, H., Moskaug, J. O., Fromm, S. H., and Blomhoff, R. (2002). In vivo imaging of NF-kappa B activity. *J Immunol* **168**(3), 1441–6.

Chung, A., Karlan, S., Lindsley, E., Wachsmann-Hogiu, S., and Farkas, D. L. (2006). In vivo cytometry: a spectrum of possibilities. *Cytometry A* **69**(3), 142–6.

Choy, G., Choyke, P., and Libutti, S. K. (2003). Current advances in molecular imaging: noninvasive in vivo bioluminescent and fluorescent optical imaging in cancer research. *Mol Imaging* **2**(4), 303–12.

Contag, C. H., Contag, P. R., Mullins, J. I., Spilman, S. D., Stevenson D. K., and Benaron D. A. (1995). Photonic detection of bacterial pathogens in living hosts. *Mol Microbiol* **18**(4), 593–603.

Conrath, J., Erginay, A., Giorgi, R., Lecleire-Collet, A, Vicaut E, Klein J. C., Gaudric, A., and Massin, P. Evaluation of the effect of JPEG and JPEG2000 image compression on the detection of diabetic retinopathy. Eye. online publication 3 February 2006; doi: 10.1038/sj.eye.6702238

Costello, S. S., Johnston, D. J., Dervan, P. A., and O'Shea1, D. G. (2003). Development and evaluation of the virtual pathology slide: a new tool in telepathology. *J Med Internet Res* **5**(2), e11.

Crawford, W. (2003). *The Scope and History of Pathology*, <http://www.usc.edu/hsc/dental/PTHL312abc/312a/01/Reader/reader.pdf>. The University of Southern California School of Dentistry, Los Angeles, CA.

De Clerck, N. M., Meurrens, K., Weiler, H., Van Dyck, D., Van Houtte, G., Terpstra, P., and Postnov, A. A. (2004). High-resolution X-ray microtomography for the detection of lung tumors in living mice. *Neoplasia* **6**(4), 374–9.

Delnomdedieu, M., Hedlund, L. W., Johnson, G. A., and Maronpot, R. R. (1996). Magnetic resonance microscopy—a new tool for the toxicologic pathologist. *Toxicol Pathol* **24**(1), 36–44.

Delnomdedieu, M., Hedlund, L. W., Maronpot, R. R., and Johnson, G. A. (1998). Magnetic resonance microscopy and histopathology: comparative approach of bromobenzene-induced hepatotoxicity in the rat. *Hepatology* **27**(2), 526–32.

Demichelis, F., Della Mea, V., Forti, S., Dalla Palma, P., and Beltrami, C. A. (2002). Digital storage of glass slides for quality assurance in histopathology and cytopathology. *J Telemed Telecare* **8**(3), 138–42.

DiIulio, R. (2006). Medical Imaging—Step-by-step: color monitor comparison chart. <http://www.medicalimagingmag.com/assets/pdf/StepByStep_March_Chart.pdf>. *Medical Imaging*, Los Angeles, CA.

Dixon, D., Johnson, G. A., Cofer, G. P., Hedlund, L. W., and Maronpot, R. R. (1988). Magnetic resonance imaging (MRI): a new tool in experimental toxicologic pathology. *Toxicol Pathol* **16**(3), 386–91.

Doyle, T. C., Burns, S. M., and Contag, C. H. (2004). In vivo bioluminescence imaging for integrated studies of infection. *Cell Microbiol* **6**(4), 303–17.

Drent, P. (2005). Properties and selection of objective lenses for light microscopy applications. *Microsc Anal* **75**, 5–7.

Felten, C. L., Strauss, J. S., Okada, D. H., and Marchevsky, A. M. (1999). Virtual microscopy: high resolution digital photomicrography as a tool for light microscopy simulation. *Hum Pathol* **30**, 477–83.

Gagnon, M., Inhorn, S., Hancock, J., Keller, B., Carpenter, D., Merlin, T., Hearn, T., Thompson, P., and Whalen, R. (2004). Comparison of cytology proficiency testing: glass slides vs. virtual slides. *Acta Cytol* **48**(6), 788–94.

Gambhir, S. S., Herschman, H. R., Cherry, S. R., Barrio, J. R., Satyamurthy, N., Toyokuni, T., Phelps, M. E., Larson, S. M., Balatoni, J., Finn, R., Sadelain, M., Tjuvajev, J., and Blasberg, R. (2000). Imaging transgene expression with radionuclide imaging technologies. *Neoplasia* **2**(1–2), 118–38.

Gasser, J. A., Ingold, P., Grosios, K., Laib, A., Hammerle, S., and Koller, B. (2005). Noninvasive monitoring of changes in structural cancellous bone parameters with a novel prototype micro-CT. *J Bone Miner Metab* **23**(Suppl 1), 90–6.

Giuliano, K. A., and Taylor, D. L. (1998). Fluorescent-protein biosensors: new tools for drug discovery. *Trends Biotechnol* **16**(3), 135–40.

Haka, A. S., Volynskaya, Z., Gardecki, J. A., Nazemi, J., Lyons, J., Hicks, D., Fitzmaurice, M., Dasari, R. R., Crowe, J. P., and Feld, M. S. (2006). In vivo margin assessment during partial mastectomy breast surgery using Raman spectroscopy. *Cancer Res* **66**(6), 3317–22.

Hedlund, L. W., Maronpot, R. R., Johnson, G. A., Cofer, G. P., Mills, G. I., and Wheeler, C. T. (1991). Magnetic resonance microscopy of toxic renal injury induced by bromoethylamine in rats. *Fundam Appl Toxicol* **16**(4), 787–97.

Helin, H. O., Lundin, M. E., Laakso, M., Lundin, J., Helin, H. J., and Isola, J. (2006). Virtual microscopy in prostate histopathology: simultaneous viewing of biopsies stained sequentially with hematoxylin and eosin, and alpha-methylacyl-coenzyme a racemase/p63 immunohistochemistry. *J Urol* **175**(2), 495–9.

Hendee, W. R., and Ritenour, E. R. (2002). *Medical Imaging Physics* (4th ed.). Wiley-Liss, New York.

Herschman, H. R. (2003). Molecular imaging: looking at problems, seeing solutions. *Science* **302**, 605–08.

Hockings, P. D., Changani, K. K., Saeed, N., Reid, D. G., Birmingham, J., O'Brien, P., Osborne, J., Toseland, C. N., and Buckingham, R. E. (2003). Rapid reversal of hepatic steatosis, and reduction of muscle triglyceride, by rosiglitazone: MRI/S studies in Zucker fatty rats. *Diabetes Obes Metab* **5**(4), 234–43.

Hoffman, R. M. (2002). Green fluorescent protein imaging of tumour growth, metastasis and angiogenesis in mouse models. *Lancet Oncol* **3**, 546–56.

Hoffman, R. M. (2004). Imaging tumor angiogenesis with fluorescent proteins. *APMIS* **112**(7–8), 441–9.

Hoffman, R. M. (2005). Advantages of multi-color fluorescent proteins for whole-body and in vivo cellular imaging. *J Biomed Opt* **10**(4), 412001-10.

Jerry, L., Prince, J. L., and Links, J. (2005). *Medical Imaging Signals and Systems*. Prentice Hall, Upper Saddle River, NJ.

Johnson, G. A., Cofer, G. P., Fubara, B., Gewalt, S. L., Hedlund, L. W., and Maronpot, R. R. (2002). Magnetic resonance histology for morphologic phenotyping. *J Magn Reson Imaging* **16**(4), 423–9.

Johnson, G. A., and Maronpot, R. R. (1989). Magnetic resonance microscopy of chemically-induced liver foci. *Toxicol Pathol* **17**(4 Pt 1), 613–6.

Johnson, P. C., and Braughler, J. M. (2003). Automated pathology in toxicology and drug safety. *Curr Drug Discov* **3**(12), 23–8.

Kriete, A., and Boyce, K. (2003). Advanced tissue analysis using a combined histomorphometric and gene expression profiling method. *SPIE Proc* Vol. 4958, Bellingham.

Kriete, A., and Boyce, K. (2005). Automated tissue analysis—a bioinformatics perspective. *Meth Inf Med* **44**(1), 32–7.

Kumar, R. K., Velan, G. M., Korell, S. O., Kandara, M., Dee F. R., and Wakefield, D. (2004). Virtual microscopy for learning and assessment in pathology. *J Pathol* **204**(5), 613–8.

Laforest, R., Sharp, T. L., Engelbach, J. A., Fettig, N. M., Herrero, P., Kim, J., Lewis, J. S., Rowland, D. J., Tai, Y. C., and Welch, M. J. (2005). Measurement of input functions in rodents: challenges and solutions. *Nucl Med Biol* **32**(7), 679–85.

Langheinrich, A. C., Leithauser, B., Greschus, S., Von Gerlach, S., Breithecker, A., Matthias, F. R., Rau, W. S., and Bohle, R. M. (2004a). Acute rat lung injury: feasibility of assessment with micro-CT. *Radiology* **233**(1), 165–71.

Langheinrich, A. C., Bohle, R. M., Breithecker, A., Lommel, D., and Rau, W. S. (2004b). Micro-computed tomography of the vasculature in parenchymal organs and lung alveoli. *Rofo* **176**(9), 1219–25.

Lee, T. C., Mohsin, S., Taylor, D., Parkesh, R., Gunnlaugsson, T., O'Brien, F. J., Giehl, M., and Gowin W. (2003). Detecting microdamage in bone. *J Anat* **203**(2), 161–72.

Leong, F. J., and Leong, A. S. (2004). Digital imaging in pathology: theoretical and practical considerations, and applications. *Pathology* **36**(3), 234–41.

Lundin, M., Lundin, J., Helin, H., and Isola, J. (2004). A digital atlas of breast histopathology: an application of web-based virtual microscopy. *J Clin Pathol* **57**, 1288–91.

Magness, S. T., Jijon, H., Van Houten Fisher, N., Sharpless, N. E., Brenner, D. A., and Jobin, C. (2004). In vivo pattern of lipopolysaccharide and anti-CD3-induced NF-kappa B activation using a novel gene-targeted enhanced GFP reporter gene mouse. *J Immunol* **173**(3), 1561–70.

Malaisse, W. J. (2005). Non-invasive imaging of the endocrine pancreas (review). *Int J Mol Med* **15**(2), 243–6.

Malkin, H. M. (1998). History of pathology: comparison of the use of the microscope in pathology in Germany and the United States during the nineteenth century. *Ann Diagn Pathol* **2**(1), 79–91.

Maronpot, R. R., Sills, R. C., and Johnson, G. A. (2004). Applications of magnetic resonance microscopy. *Toxicol Pathol* **32**(Suppl 2), 42–8.

McCullough, B., Ying, X., Monticello, T. M., and Bonnefoi, M. (2004). Digital microscopy imaging and new approaches in toxicologic pathology. *Toxicol Pathol* **32**(Suppl 2), 49–58.

Molnar, B., Berczi, L., Diczhazy, C., Tagscherer, A., Varga, S. V., Szende, B., and Tulassay, Z. (2003). Digital slide and virtual microscopy based routine and telepathology evaluation of routine gastrointestinal biopsy specimens. *J Clin Pathol* **56**(6), 433–8.

Montet, X., Ntziachristos, V., Grimm, J., and Weissleder, R. (2005). Tomographic fluorescence mapping of tumor targets. *Cancer Res* **65**(14), 6330–36.

Morgan, D. L., Little, P. B., Herr, D. W., Moser, V. C., Collins, B., Herbert, R., Johnson, G. A., Maronpot, R. R., Harry, G. J., and Sills, R. C. (2004). Neurotoxicity of carbonyl sulfide in F344 rats following inhalation exposure for up to 12 weeks. *Toxicol Appl Pharmacol* **200**(2), 131–45.

Myers, R. (2001). The biological application of small animal PET imaging. *Nucl Med Biol* **28**, 585–93.

Nixon, E., Recheis. W., Ross, A., Auger, M., Ying, X., Underwood, S. Schmidt, J., DeSanctis, G. T., and Hoffman, E. A. (2005). In vivo and ex vivo micro-CT of the mouse airway wall. *ATS*, San Diego, CA.

Oakley, J. (2003). *Digital Imaging: A Primer for Radiographers, Radiologists and Health Care Professionals*. Cambridge University Press, Cambridge, UK.

Okada, D. H., Binder, S. W., Felten, C. L., Strauss, J. S., and Marchevsky, A. M. (1999). "Virtual microscopy" and the Internet as telepathology consultation tools: diagnostic accuracy in evaluating melanocytic skin lesions. *Am J Dermatopathol* **21**(6), 525.

Okumura, A., Suzuki, J., Furukawa, I., Ono, S., and Ashihara, T. (1997). Signal analysis and compression performance evaluation of pathological microscopic images. *IEEE Trans Med Imaging* **16**(6), 701–10.

Olszak, A. G., and Descour, M. R. (2005). Microscopy in multiples. *OE Mag* **5**(5), 16–8.

Pawley, J. B. (2006). *Handbook of Biological Confocal Microscopy* (3rd ed). Plenum Press, New York.

Piller, G. J. (2001). Leukaemia—a brief historical review from ancient times to 1950. *Bri J Haematol* **112**, 282–92.

Pinaud, F., Michalet, X., Bentolila, L. A., Tsay, J. M., Doose, S., Li, J. J., Iyer, G., and Weiss, S. (2006). Advances in fluorescence imaging with quantum dot bio-probes. *Biomaterials* **27**(9), 1679–87.

Postnov, A. A., Meurrens, K., Weiler, H., Van Dyck, D., Xu, H., Terpstra, P., and De Clerck, N. M. (2005). In vivo assessment of emphysema in mice by high resolution X-ray microtomography. *J Microsc* **220**(Pt 1), 70–5.

Preece, N. E., Houseman, J., King, M. D., Weller, R. O., and Williams, S. R. (2004). Development of vigabatrin-induced lesions in the rat brain studied by magnetic resonance imaging, histology, and immunocytochemistry. *Synapse* **53**(1), 36–43.

Preston, K. Jr. (1986). High-resolution image analysis. *J Histochem Cytochem* **34**(1), 67–74.

Ritman, E. L. (2002). Molecular imaging in small animals—roles for micro-CT. *J Cell Biochem Suppl* **39**, 116–24.

Ritman, E. L. (2005). Micro-computed tomography of the lungs and pulmonary-vascular system. *Proc Am Thorac Soc* **2**(6), 477–80, 501.

Rossner, M., and O'Donnell, R. (2004). The JCB will let your data shine in RGB. *J Cell Biol* **164**, 11–3.

Rubart, M. (2004). Two-photon microscopy of cells and tissue. *Circ Res* **95**(12), 1154–66.

Rudin, M., and Weissleder, R. (2003). Molecular imaging in drug discovery and development. *Nat Rev Drug Discov* **2**, 123–31.

Samei, E., et al. (2005). Assessment of display performance for medical imaging systems. <http://www.aapm.org/pubs/reports/OR_03.pdf>. American Association of Physicists in Medicine, College Park, MD.

Seeram, E. (1994). *Computed Tomography: Physical Principles, Clinical Applications, and Quality Control* (1st ed). W. B. Saunders Company, Philadelphia, PA.

Schmitz, S. A., Muhler, A., Wagner, S., and Wolf, K. J. (1996). Functional hepatobiliary imaging with gadolinium-EOB-DTPA. A comparison of magnetic resonance imaging and ^{153}gadolinium-EOB-DTPA scintigraphy in rats. *Invest Radiol* **31**(3), 154–60.

Shah, K., and Weissleder, R. (2005). Molecular optical imaging: applications leading to the development of present day therapeutics. *NeuroRx* **2**(2), 215–25.

Shotton, D. (1993). *Electronic Light Microscopy*. John Wiley & Sons., New York.

Singer, R. H., Lawrence, D. S., Ovryn, B., and Condeelis, J. (2005). Imaging of gene expression in living cells and tissues. *J Biomed Opt* **10**(5), 051406.

Steinberg, D. M., and Ali, S. Z. (2001). Application of virtual microscopy in clinical cytopathology. *Diagn Cytopathol* **25**(6), 389–396.

Suetens, P. (2002). *Fundamentals of Medical Imaging*. Cambridge University Press, Cambridge, UK.

Tengowski, M. W. (2004). Image compression in morphometry studies requiring 21 CFR Part 11 compliance: procedure is key with TIFFs and various JPEG compression strengths. *Toxicol Pathol* **32**(2), 258–63.

Tengowski, M. W., and Kotyk, J. J. (2005). Risk identification and management: MRI as a research tool in toxicology studies of new chemical entities. *Prog Drug Res* **62**, 257–78.

Wang J., and Maurer L. (2005). Positron Emission Tomography: applications in drug discovery and drug development. *Curr Top Med Chem* **5**(11), 1053–75.

Weinstein, R. S., Descour, M. R., Liang, C., Barker, G., Scott, K. M., Richter, L., Krupinski, E. A., Bhattacharyya, A. K., Davis, J. R., Graham, A. R., Rennels, M., Russum, W. C., Goodall, J. F., Zhou, P., Olszak, A. G., Williams, B. H., Wyant, J. C., and Bartels, P. H. (2004). An array microscope for ultrarapid virtual slide processing and telepathology. Design, fabrication, and validation study. *Hum Pathol* **35**(11), 1303–14.

Weinstein, R. S., Descour, M. R., Liang, C., Richter, L., Russum, W. C., Goodall, J. F., Zhou, P., Olszak, A. G., and Bartels, P. H. (2005). Reinvention of light microscopy: array microscopy and ultrarapidly scanned virtual slides for diagnostic pathology and medical education. In: Virtual Microscopy and Virtual Slides in Teaching, Diagnosis and Research (Gu, J. & Ogilvie, R. W., eds.), pp. 9–35, CRC Press, Taylor & Francis, Boca Raton, FL.

Weir, L. R., Schenck, E., Meakin, J., McClure, F., Driver, R., Walker, S., and Lynch, A. M. (2005). Biophotonic imaging in HO-1.luc transgenic mice: real-time demonstration of gender-specific chloroform induced renal toxicity. *Mutat Res* **574**(1–2), 67–75.

Weiss, K. L., Schroeder, C. E., Kastin, S. J., Gibson, J. P., Yarrington, J. T., Heydorn, W. E., McBride, R. G., Sussman, N. M., and Arezzo, J. C. (1994). MRI monitoring of vigabatrin-induced intramyelinic edema in dogs. *Neurology* **44**(10), 1944–9.

Welsh, D. K., and Kay S. A. (2005). Bioluminescence imaging in living organisms. *Curr Opin Biotechnol* **16**(1), 73–8.

Wetzel, A. W., Gilbertson, J. R., Beckstead, J. A., Feineigle, P. A., Hauser, C. R., and Palmieri, F. A. (2006). System and method for finding regions of interest for microscopic digital montage imaging. <US Patent #6993169. http://patft.uspto.gov/netahtml/srchnum.htm>.

Wootton, R., Springall, D. R., and Polak, J. M. (1995). *Image Analysis in Histology—Conventional and Confocal Microscopy*, Cambridge University Press, London.

Ying, X. (1995). Digital imaging based measurements and analyses in quantitative biomedical research at cellular and microvascular levels. *Acta Univ. Oul*., A272 (ISBN 951-42–4245-9), Oulu, Finland.

Ying, X., and Chung, L. (1999). Image file formats for digital microscopy. *Microsc & Anal* **34**, 9–11.

Ying, X., Bienvenu, J-G., Pino, M., and Monticello, T. M. (2004). Application of digital (virtual) slide microscopy in toxicologic pathology (poster presentation #P57), *STP Annual Meeting*, Salt Lake City, UT.

Yee, S. H., Jerabek, P. A., and Fox, P. T. (2005). Non-invasive quantification of cerebral blood flow for rats by microPET imaging of 15O labelled water: the application of a cardiac time-activity curve for the tracer arterial input function. *Nucl Med Commun* **26**(10), 903–11.

Zhang, X., Tengowski, M., Fasulo, L., Botts, S., Suddarth, S. A., and Johnson, G. A. (2004). Measurement of fat/water ratios in rat liver using 3D three-point dixon MRI. *Magn Reson Med* **51**(4), 697–702.

Zhou, X., Maronpot, R. R., Cofer, G. P., Hedlund, L. W., and Johnson, G. A. (1994). Studies on bromobenzene-induced hepatotoxicity using in vivo MR microscopy with surgically implanted RF coils2 *Magn Reson Med* **31**(6), 619–27.